Available online at www.sciencedirect.com

jmr&t Journal of Materials Research and Technology

journal homepage: www.elsevier.com/locate/jmrt

Original Article

Bio-inspired self-healing of concrete cracks using new B. pseudomycoides species

Hassan Amer Algaifi [a,*], *Suhaimi Abu Bakar* [b], *Rayed Alyousef* [c,**], *Abdul Rahman Mohd Sam* [b], *M.H. Wan Ibrahim* [a,***], *Shahiron Shahidan* [a], *Mohammed Ibrahim* [d], *Babatunde Abiodun Salami* [d]

[a] *Faculty of Civil Engineering and Built Environment, Universiti Tun Hussein Onn Malaysia, Parit Raja, Johor, 86400, Malaysia*

[b] *School of Civil Engineering, Faculty of Engineering, Universiti Teknologi Malaysia, 81310, Johor Bahru, Johor, Malaysia*

[c] *Department of Civil Engineering, College of Engineering, Prince Sattam Bin Abdulaziz University, Al-Kharj, 11942, Saudi Arabia*

[d] *Center for Engineering Research, Research Institute, King Fahd University of Petroleum and Minerals, Dhahran, 31261, Saudi Arabia*

ARTICLE INFO

Article history:
Received 9 December 2020
Accepted 8 March 2021
Available online 14 March 2021

Keywords:
Bacterial concrete
X-ray computed microtomography
Self-healing concrete
Concrete strength
Bio-inspired self-healing

ABSTRACT

Bio-inspired self-healing of concrete cracks has been widely exploited to improve concrete properties and thus increase concrete life span using different bacterial species in recent years. The most common bacterial species found in the present literature are *B. sphaericus*, *Sporosarcina pasteurii*, Spore-forming alkali-resistant bacteria, *B. megaterium* and *B. subtilis*, while there is no published research using *B. pseudomycoides* species to heal concrete cracks. Furthermore, the need for more in-depth information on the healing ratio in the deeper part of the concrete crack remains. In the present study, a new bacterial species, namely *B. pseudomycoides* strain HASS3, was isolated, identified and tested for its ability to heal artificially cracked concrete samples. Both variable-pressure scanning electron microscope (VP-SEM) and X-ray computed microtomography (X-ray μCT) were utilised to assess the evolution of the healing ratio along with the crack profile. VP-SEM results revealed that a crack mouth width of 0.4 mm was fully healed through microbial precipitation which was later identified as calcite and vaterite using XRD. In contrast, according to the X-ray μCT results, the maximum healing ratio in the deeper part of the crack was only 14% compared to the crack mouth. As such, it could be concluded that bacteria-based concrete self-healing could function as a sustainable strategy to heal cracks located in the concrete skin.

* Corresponding author.
** Corresponding author.
*** Corresponding author.
E-mail addresses: enghas78@gmail.com (H.A. Algaifi), r.alyousef@psau.edu.sa (R. Alyousef), haziman@uthm.edu.my (M.H.W. Ibrahim).

https://doi.org/10.1016/j.jmrt.2021.03.037

1. Introduction

Concrete cracks are almost inevitable. This is unsurprising, as concrete matrix has been relatively regarded for its brittleness and heterogeneity [1,2]. These cracks can be created even without any external load from early-age thermal gradient, bleeding, shrinkage, expensive reaction and so on [3–5]. Given this, the formation and existence of concrete microcracks, especially in the concrete skin, continues to be a present-day concern and challenge for civil engineers globally [6]. This is because the microcracks can facilitate the ingress of aggressive material and thus deteriorate the concrete structure [7,8]. As such, developing smart and sustainable concrete is in urgent demand in order to control the propagation of cracks and heal them as fast as possible [9]. In recent years, sustainable concrete technology, specifically the topic of self-healing concrete has become research hotspot [10]. In general, the aim of the self-healing of concrete cracks is to improve and densify the concrete skin, thus extending the life span of concrete structures and simultaneously reducing the maintenance cost expended on cement-based structural deterioration [11]. There are several methods of concrete self-healing that are presently available in the literature, such as, using crystalline admixtures [12–14], polymer-based [15,16] and bacteria-based [17,18]. From the point of bacteria-based self-healing, the healing mechanism was inspired from the remarkable bio-healing of the human wounds. Relatedly, injured human skin would call upon platelets, which are uniformly distributed in the blood, toward the injured area. Subsequently, the platelets would clot the blood, thus stopping the bleeding.

Consequently, several innovative techniques have been exploited to heal concrete cracks such as shape memory alloy [19], mineral admixture [20,21], superabsorbent polymers [22–24] and silica-based material [25,26]. In addition, many researchers have also devoted significant effort in order to introduce a sustainable self-healing technique using different metabolic bacterial activity such as sulfate reduction bacteria [27], nitrate reduction bacteria [28,29], oxidation of organic acids [30] and hydrolysis of urea [31,32]. Of the aforementioned, the most commonly used healing mechanism is the hydrolysis of urea via ureolytic bacteria. In addition, most of the bacterial species used in the literature included *B. sphaericus* [33–35], *B. subtilis* [36,37], *Sporosarcina pasteurii* [38], and *B. megaterium* [39]. Regardless, there is little attention focused on the investigation of the healing efficiency in the deeper part of concrete cracks; instead, the healing efficiency were mostly investigated either by roughly quantifying the precipitation of calcium carbonate using photographic imaging [40–45], or using indirect techniques such as mechanical and durability tests [46,47].

For the same regard [45], demonstrated that *Bacillus alkalinitrilicus* species was able to close a 0.4 mm crack after 100 days, while, 0.18 mm-wide cracks were healed in the control concrete specimen without bacteria owing to autogenous self-healing. The healing was attributed to the microbial calcium carbonate precipitation by the metabolic activity of the bacteria. In a separate study [48], used *B. sphaericus* to induce microbial product in cracked concrete specimens in which a crack width of 0.5 mm was completely filled after 7 days. Moving to nitrate reduction bacteria [28], anaerobic bacterium was used with no oxygen requirement for growth to densify concrete microstructure through microcracks and pores filling inside the concrete matrix. Based on their results, a 0.48 mm crack width was fully healed after 56 days through the precipitation of $CaCO_3$ and its concentration was located close to the surface. In the same context, a crack width of 0.79 mm was fully healed using *B. cohnii*, species in a study reported by [49]. Other bacterial species used are also available in the present literature [50–59].

It could be inferred that researchers are still devoting great efforts to enhance the precipitation of microbial calcium carbonate inside the cement-based material by using different bacterial species. In the present study, a novel native bacterial species, *B. pseudomycoides* strain HASS3, was isolated and used to heal cracked concrete samples. The influence of the bacteria on concrete strength was first evaluated. Then, variable-pressure scanning electron microscope (VP-SEM) and X-ray computed microtomography (X-ray μCT) were used to examine the evolution of $CaCO_3$ precipitation at the crack mouth and the deeper part of the crack, respectively.

2. Experimental program

2.1. Bacterial isolation and identification

A new bacterial species was isolated from a soil sample which was collected from Universiti Teknologi Malaysia (UTM) grounds. One gram of the soil sample was submerged in 25 mL of lysogeny broth (LB) for 24 h in order to grow the bacteria that lay around the soil. Then, the streak plate technique was used to separate each single bacterium from the others [60]. In other words, each single bacterium would grow and reproduce forming a colony on the Petri dish. It is interesting to note that each bacterium has its own appearance such as shape, size and colour. In addition, the colony morphology was observed with the naked eye, as colony morphology is not difficult to recognise.

Standard Gram stain was also considered to determine the isolated bacteria whether it belonged to *Bacillus* gene or otherwise. The process of gram stain test mimicked the work of [61]. Meanwhile, endospore formation was carried out in reference to a study by [39] which was conducted to check for the potential ability of the isolated bacteria to produce spore.

In the same regard, the morphology of the isolated bacteria were also investigated using VP-SEM in order to examine its shape and size. In the first step, the isolated bacteria was cultured overnight. Subsequently, it was harvested with a centrifuging instrument. Next, using a microcentrifuge tube, it was washed twice with distilled water (dH_2O). Later, the bacteria cells were harvested again and rinsed with dH_2O. Later,

the target sample was moved to cover glasses (Fisher Scientific), which was coated with Poly-lysine to facilitate the adhesion between the bacteria cells and glass. Then, the bacteria were fixed by adding 1 mL of 2.5% glutaraldehyde solution. Subsequently, the sample was immersed in hexamethyldisilazane for 2 h. Lastly, it was stored in a desiccator overnight to enable the bacterial cells to dry. In addition, the isolated bacteria was also tested for urease activity in order to differentiate whether it belonged to ureolytic or non-ureolytic bacteria using the Nessler method, as discussed in the next section.

2.2. Ureolytic activity

To examine the ureolytic activity, the isolated bacteria was first cultured in a 100 mL flask containing 30 mL LB and 6 mM urea. Then, it was incubated at 37 °C for 24 h. Next, 0.1 mL of the urea-LB culture was taken and tested to measure its ammonia concentration using the Nessler Method 8038. Indeed, Nessler reagent is regarded as a colour creation reagent and is widely used in the literature [62,63]. Generally, it is an alkaline solution of potassium tetraiodo mercurate complex compound and would react with ammonia ions to induce a yellow colour in the medium. In this study, the absorbance and intensity of the yellow colour was analysied using UV–Vis Spectrophotometer (Hach, Model 5000) and converted using Lambert–Beer Law to represent the ammonia concentration in the specimen (mg/L).

The presence and amount of ammonia would indicate that the isolated bacteria has the ability to produce urease enzyme which is the sole parameter to decompose urea into carbonate and ammonia. The amount of urea decomposition was calculated using Eq. (1) [64]. In addition, the logistic curve fitting was adopted in order to calculate the rate of urea hydrolysis as shown in Eq. (2). Where, y was the experimental urea hydrolysis at time t, c was the time at the maximum of (dy/dt), k_1 was the reaction rate constant and a was the range of y.

$$urea\ decomposed(mg/L) = \frac{NH_{3(mg/L)} \times 60_{(g/mol)}}{2 \times 17_{(g/mol)}} \quad (1)$$

$$y = \frac{a}{1 + e^{-k_1(x-c)}} \quad (2)$$

2.3. DNA identification of the isolated bacteria

DNA identification is important as it functions because it is a type of genetic fingerprinting. It provides insight into the species and strains name using the bacterial genetic code 16 S rRNA [65]. Four steps were taken into account to obtain the pure DNA, namely extraction, PCR amplification, purification and sequencing. Firstly, the DNA from overnight cultures of the isolated bacteria were extracted using the Promega Genomic Wizard DNA Purification Kit (Promega, Madison, WI, USA). Then, both the yield and purity of the extracted DNA were assessed using the Nano Drop spectrophotometer (Thermo Scientific, 1000 Model) prior to the PCR amplification. Subsequently, the Promega PCR kit procedure was followed to clone the specific region of the specific gene DNA which was 16s rRNA. The reaction specimen of 50 μL included 25 μL target DNA, 1 μL Master mix (containing dNTPs, Taq DNA polymerase, MgCl2 and reaction buffers), 1 μL forward primer (Fd1) 5′-AGA GTT TGA TCC TGG CTC AG-3′, 1 μL reverse primer (rP1) 5′-ACG GCT ACC TTG TTA CGA CTT-3′ and 22 μL distilled water. Different temperatures for a certain period of time (cycles) were taken into account to implement the PCR reaction through the Mastercycler nexus instrument (Eppendorf). Next, based on the protocol specified in the QIAquick PCR purification (Qiagen), the new nucleotide DNA (PCR product) was purified. To evaluate the purity and concentration of the amplified 16 S rRNA, the PCR product was also electrophoresed in 1% (w/v) agarose gel. Next, the amplified 16 S RNA gene was sequenced (Sanger sequencing) in First Base Laboratory Sdn. Bhd. In addition, the result of the sequence data was analysed in the National Centre for Biotechnology Information (NCBI) using a blast program. Finally, the 16 s rRNA gene sequences were deposited in the gene bank database (Gene Accession No. MK357893).

2.4. Concrete strength

The concrete compressive strength was assessed to understand how much the bacterial solution would affect the concrete strength. Two mixes were set, namely (1) control concrete mix and (2) bacterial concrete mix with the bio-based healing agent. The design of the control concrete mix (without the bio-based healing agent) was based on the Department of Environment (DOE) method of British specification to obtain a concrete strength of 30 MPa after 28 days. Ordinary Portland Cement (OPC), local natural sand, crushed granite (10 mm) and Rheobuild 1100 super plasticiser were used for this purpose.

For the bacterial concrete mix, the bio-based healing agent (bacterial solution, urea and calcium nitrate tetrahydrate) was prepared and added to the mixing water. Pertaining to the bacterial solution, the isolated bacteria were cultured in 100 mL Erlenmeyer flasks filled with 30 mL of LB at 32 °C and 150 rpm. It should be noted that the incubation period was kept at 2 weeks to ensure that the bacterial spores are formed. This was in line with [64] who stated that 90% of the bacterial cells would be converted into spores when the incubation period of the bacterial culture is more than two weeks. In addition, 0.01 g/L of $MnSO_4.H_2O$ was added to enhance the spore formation. After that, the optical density (OD_{600}) was found to be 2.1 using a spectrophotometer (Jenway 7305 UV/Visible). Later, the value of OD_{600} was converted to represent the bacterial spore concentration (2.3×10^8 cells/mL) using Eq. (3) [66]. Where, Y was the cells concentration (cells/mL) and X represented the optical density value. In the same context, according to [67]; the bacterial solution was diluted to achieve a bacterial cells concentration of 2×10^7 cells/mL in the concrete mixing water. This is because the excessive amount of bacterial broth, that involves nutrient (3 g/L) and bacterial cells, would hinder cement hydration reaction and thus affect the concrete strength. In addition, the used dilution formula as is described in Eq. (4) [68]. Where, C_1 and V_1 were the concentration and volume of the bacterial solution respectively. In addition, the concentration and volume of the target mixing water were represented by C_2 and V_2 respectively.

Table 1 – Concrete mixing properties.

	Ingredient							
	Cemen	Water (L)	Coarse aggregate	Fine aggregate	admixture (L)	Urea	calcium nitrate	Bacterial solution (L)
Mass (kg/m^3)	425	235	620	1100	5.1	4.7	2.35	20.43

$$Y = 8.59 \times 10^7 X^{1.3627} \quad (3)$$

$$C_1 \times V_1 = C_2 \times V_2 \quad (4)$$

On the other hand, urea concentration of 20 g/L was added into the mixing water. While, the concentration of calcium nitrate tetrahydrate was 250 Mm. The molarity of both the urea and calcium nitrate tetrahydrate were calculated using Eq. (5). Table 1 describes the details of the bacterial concrete mixed used.

$$\text{Molarity } (M) = \frac{\text{moles of solute}}{\text{liters of solution}} = \frac{\text{weight}_{(g)}}{\text{volume}_{(L)} \times \text{molar mass}_{(g/M)}} \quad (5)$$

2.5. *Preparation of the artificial cracked concrete specimen*

A small specimen (mm-sized) of an artificial cracked mortar specimen was taken into account to represent the concrete matrix in the present study. The procedure of mortar casting followed BS EN 196–1:1995. In particular, the cement to sand ratio was 1:3 by mass. In addition, the water cement ratio (0.6) was kept constant even after the replacement with the bacterial solution. The bio-based healing agent were added into the mixing water in the similar manner of the concrete mix design as previously discussed in section 2.4. Following that, plastic moulds of (Φ30, 50 mm) were used to hold the mixing mortar. In addition, Groove was generated during the casting time by placing a copper plate of 0.4 mm. It is interesting to note that the insertion depth was 20 mm from the surface and was removed after 24 h. Moreover, the target specimen was cured by water submersion after 24 h in order to create the healing process. It should be noted that the temperature of the water was 30 °C that simulates the surrounding tropical temperature and the pH was 7.8. To evaluate and examine the crack healing evolution, the bio-mortar specimen was monitored every two weeks using VP-SEM. In addition, the deeper part of concrete crack was examined using X-rays μCT scan. X-rays micro computed tomography (X-rays μCT) has a positive reputation in engineering applications such as porosity profile of a material. In the present study, the X-rays μCT scan approach was carried out at Universiti Teknologi Petronas (UTP) Malaysia.

Specifically, X-rays μCT (InspeXio SMX-225CT; Shimadzu, Japan) was used to evaluate the extent and quantification of the healing ratio in the deeper part of the crack zone. The target sample was positioned between the X-ray detector (digital camera) and X-ray source (cone beam) as shown in Fig. 1. To obtain quality images, the output voltage used was increased up to 190 kV with the ampere of 100 mA. Then, the sample was rotated 360° to create 1800 views in order to improve details and resolution. The average count was kept at 16 every rotation angle (optimized signal to noise ratio) and the thickness of slice was 0.269 mm. Subsequently, VGStudio Max 3D rendering program was used to analyse 3D constructed slices. Finally, myvgl33 reader software was used to observe a horizontal cut section and analyse the precipitation of microbial product along the crack profile.

2.6. *VP-SEM-EDS and XRD*

In the present study, variable-pressure scanning electron microscope was used to monitor and observe the healing precipitation on the crack surface every two weeks. Moreover, EDX analysis was taken into account to identify the filling product using VP-SEM-EDX (Model JEOL JSM-IT300LV). On the other hand, X-rays powder diffraction (XRD) was also used to identify the precipitation product that was deposited on the

Fig. 1 – X rays CT test for bacterial mortar sample.

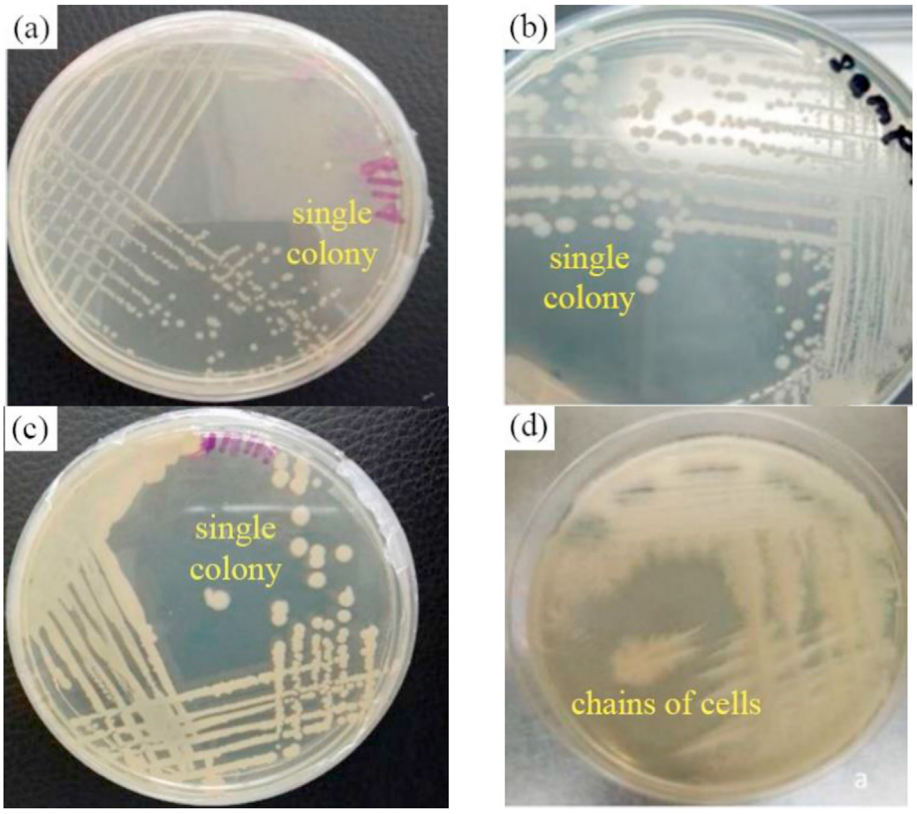

Fig. 2 – Colony morphology of all isolated bacteria (a) H1 (b) H2 (c) H3 and (d) H4 strain.

crack surface after the healing was completed. Then, the healing product was grinded into fine powder and tested using XRD (Model Rigoku). In order to induce intensive X-rays spectra, it was operated at 45 kV and 35 mA with Cu annode. In addition, the diffracted patterns were collected using D/teX Ultra 250 detector over Bragg angle (2 theta3 - 100), 8.2551 deg/min, 0.0200 deg/step as continuous scans for 10 min.

3. Results and discussion

3.1. *Bacterial strain*

Four pure bacterial colonies with different morphologies were successfully isolated from 1 g of soil specimen, which was collected from Universiti Teknologi Malaysia (UTM) grounds, as shown in Fig. 2 (a), (b),(c) and (d). It could be seen that each bacterium showed its own colony size, shape and colour. Of the four colonies, only the fourth isolate bacterium (H4) was taken into account, while the rest were dropped out as they did not meet the criteria of the target bacteria to be used in concrete. Specifically, the first bacterium (H1) did not belong to the *Bacillus* species, bacterium (H2) could not produce spore and bacterium (H3) did not induce the urease enzyme.

It is also noteworthy that the target isolate bacteria (H4) could be differentiated by its ability to form chain of cells as shown in Fig. 2d. It is common knowledge that the previously isolated *Bacillus* bacteria was grown as a single colony in a Petri dish, whereas, in the present study the isolated bacteria were grown closely by forming chains of cells that were connected to each other. This was an advantage in which the isolated bacteria would grow and form a thin layer that would fill any voids inside the concrete matrix. Moreover, chains of cells would have a larger area for calcium carbonate precipitation compared to a single colony [69]. also stated that this type of species has a remarkable characteristic to respond to

Fig. 3 – Morphology of the isolated bacteria using SEM.

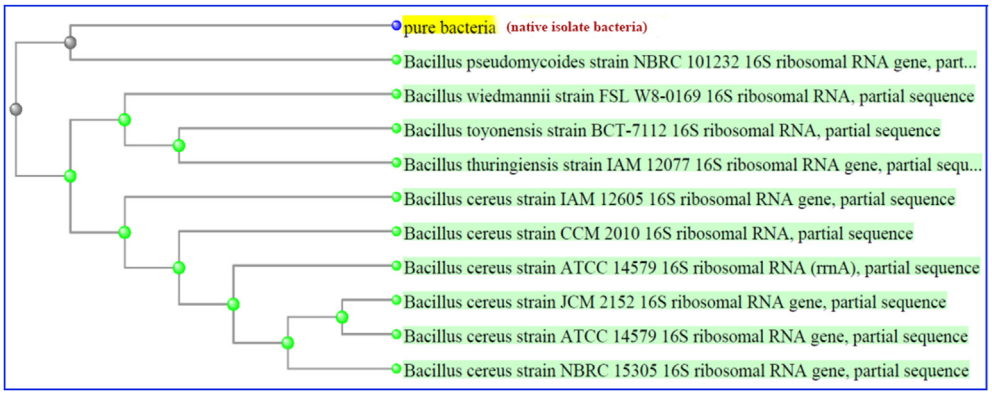

Fig. 4 – Phylogenetic tree of the isolated bacteria.

any structural deformation mechanical and force that it may face when growing in a medium.

For the same regard, the target isolated bacteria were gram-positive in which it had a rod shape as shown in Fig. 3. The length and width of the cell was found to be 4–5 μm and 1–1.5 μm respectively. Moreover, the endospore formation was also positive which enabled the bacteria to produce spore when exposed to harsh conditions such as the lack of nutrient or high pH. Both positive results were necessary for the bacteria to adopt in any harsh environment it might face. For example, it was previously acknowledged that spore is also substantial in the field of self-healing of cementitious material where the spore could resist both the mechanical and chemical stress during and after concrete mixing [30]. In the same context, gram-positive was distinguished by its thicker bacterial cell compared to gram-negative which was also necessary to sustain any stress in the concrete [70].

Moreover, the obtained 16 S rRNA gene sequence was analysed by comparing it with known bacterial sequences available in the National Centre for Biotechnology Information (NCBI). It was observed that the gene sequence of the isolated bacteria was very close to *Bacillus pseudomycoides* strain HASS3 with a similarity of 99% as shown in Fig. 4. This new species was presented and introduced as a new species to heal concrete crack in the present study. This is because the bacteria commonly used in previous studies were *S. pasteurii* [71], *Bacillus* sphaericus [34], *Bacillus* subtilis [36], *Bacillus* megaterium [67] and Spore-forming alkali-resistant bacteria [72]. Subsequently, the gene sequence of the isolated bacteria (*Bacillus pseudomycoides* strain HASS3) was deposited in the NCBI databases under the accession number of MK357893.

3.2. *Urease enzyme bacterial growth activity*

The urease enzyme test is a useful test to classify whether a particular bacterium belonged to ureolytic or non-ureolytic bacteria. The ability of the *Bacillus* pseudomycoides strain HASS3 to induce urease enzyme was proven by the presence of ammonia ions in the bacterial solution which consists of 6 mM urea concentration. This was because one mole of urease enzyme was converted into 2 mol of ammonia in the presence of urease enzyme as expressed by Eq. (6) [73]. In particular, the urease enzyme converted urea into both ammonium and carbamate. Subsequently, ammonia and carbonic acid were produced through the decomposition of carbonate as shown in Fig. 5 [74].

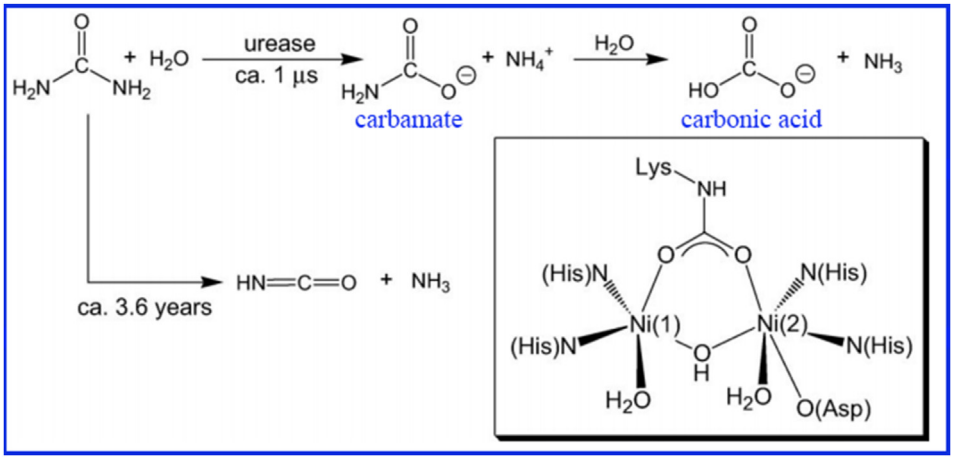

Fig. 5 – Mechanism of urea hydrolysis via urease enzyme [74].

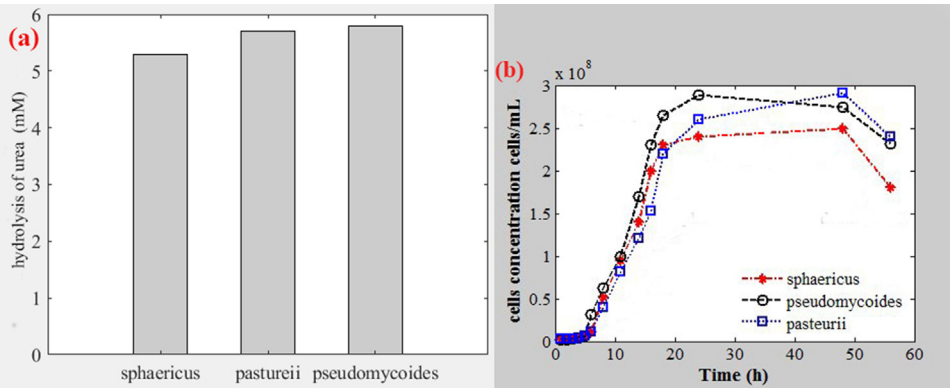

Fig. 6 – Comparison of (a) hydrolysis of urea (b) bacterial growth.

$$CO(NH_2)_2 + 2H_2O + Ca^{2+} \xrightarrow{urease} 2NH_3 + CaCO_3 \quad (6)$$

In addition, the hydrolysis efficiency of the *pseudomycoides* strain HASS3 was evaluated by comparing its productivity with other bacterial species namely, *Lysinibacillus sphaericus* HAS1 and *S. pasteurii* ATCC 11859 which was purchased from Bio-Focus Saintifik Sdn Bhd. Both of these species were chosen for comparison purposes because the *sphaericus* and *pasteurii* species have been regarded as the most effective bacterial species to be used in the field of bio-based self-healing concrete [75]. Fig. 6a shows that all bacterial species were able to hydrolyse urea into carbonate and ammonia, however, *pseudomycoides* strain HASS3 exhibited higher urea hydrolysis. It was also noticeable that no ammonia was observed in the absence of the bacteria. This fact was consistent with previously published studies which stated that the urea would be kept stable without bacteria unless the temperature increased to more than 130 °C [76]. For the concrete environment, the temperature might reach up to 70 °C [77,78]. As such, urea would not decompose inside the concrete matrix without the intervention of ureolytic bacteria. From the viewpoint of bacterial growth, the optimum growth for all bacterial species is as illustrated in Fig. 6b in which the isolate bacteria were found to be more active, compared to other bacterial species. This was because it reached its maximum concentration in just 20 h in such condition.

Going back to the hydrolysis of urea by the isolated bacteria, the rate of the urea hydrolysis though urease enzyme was calculated and evaluated using a logistic curve with a correlation coefficient of 0.98 as expressed by Eq. (7). Where y was the experimental urea concentration at time t. In particular, the rate constant of the urea hydrolysis was found to be 0.846 d^{-1}.

$$y_{(t)} = \frac{5.459}{1 + e^{-k_1(t-0.7217)}} \quad (7)$$

3.3. Concrete strength

The compressive strength of the bacterial concrete was evaluated at 7, 14 and 28 days. After 28 days, the target mean strength of the control concrete (without the bacterial solution) was 36.1 MPa. Based on the obtained results, the increase in the bacterial concrete strength was evident compared to the control specimens as shown in Fig. 7. The value of the strength enhancement was 16% higher than the control concrete. This was attributed to the precipitation of the microbial calcium carbonate inside the concrete matrix as the microbial product would fill the microcracks and the concrete pores.

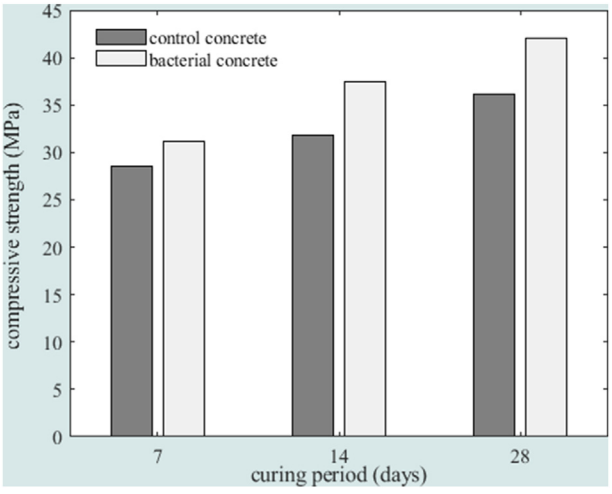

Fig. 7 – Compressive strength of the bacterial concrete at 7, 14 and 28 days.

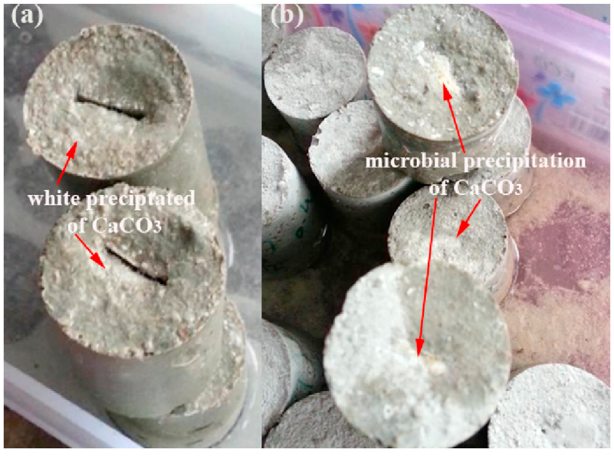

Fig. 8 – Visualisation of the healing product after 68 days (a) control mortar (b) bacterial mortar.

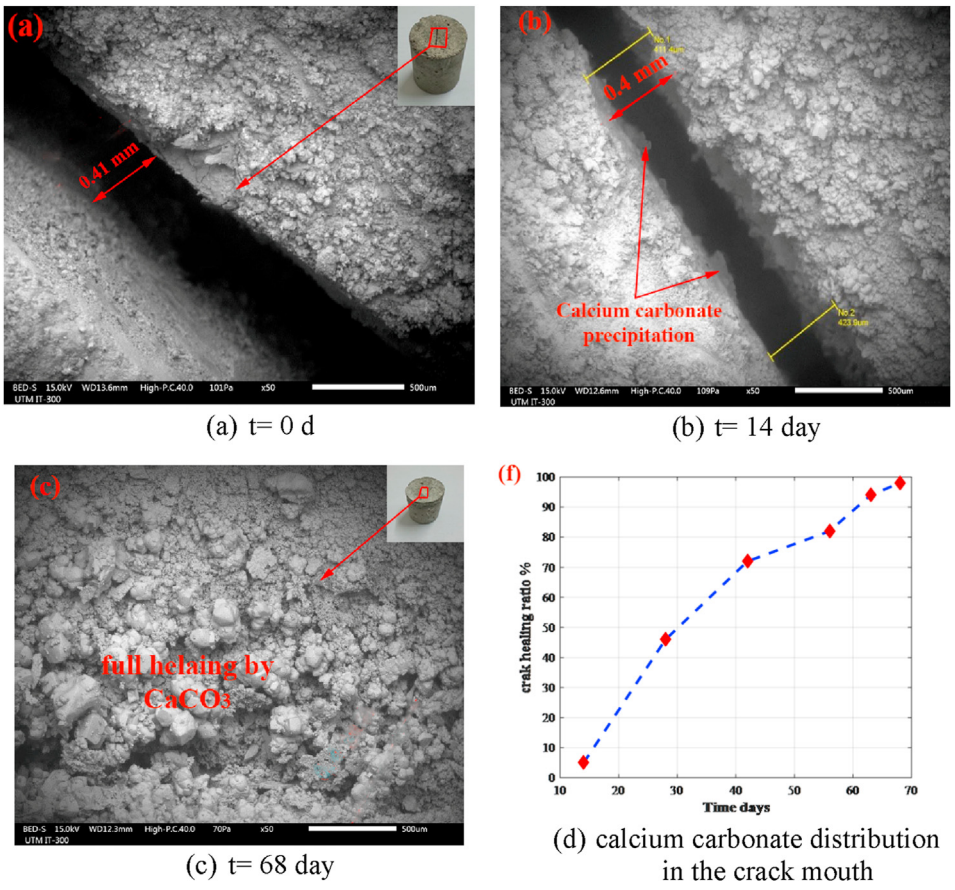

Fig. 9 – Evolution of crack healing by pseudomycoides strain HASS3.

According to [79]; the compressive strength of bacterial concrete increased by 14.8% and 34.6% when *B.* megaterium MTCC 1684 and *Lysinibacillus* sp. I13 were added respectively. Their positive finding was attributed to the deposition of calcite on the bacterial cells which in turn filled the concrete porosity. On the other hand, it could be seen that the rate of concrete strength improvement was approximately time dependent in which its enhancement was lesser at a later age as compared to the early age. This was because the concrete pores and interconnectivity paths decreased over time owing to the hydration reactions process. As such, the chemical involved such as urea faced difficulty in reaching the target area inside the concrete matrix to implement the ureolytic activity and fill the target area with calcium carbonate. Moreover, water movement and oxygen, which were substantial for ureolytic activity, were hindered due to the precipitation of calcium carbonate and continuous cement hydration [80]. From another point of view [81], stated that the viability of the bacteria was another challenging issue since the bacteria cells would be exposed to compression during the later period of time. In other words, the bacteria cell would not acquire enough space in a long run. Therefore, researchers are still focusing their efforts to develop a new carrier protection technique to encapsulate or immobilise the bacterial cell inside the concrete matrix [82]. These techniques would protect the bacteria from crushing due to the decreasing concrete pores over time.

3.4. *Evolution of bio-based crack healing*

In reference to Fig. 8a, no healing was absorbed in the control cracked mortar specimen of 0.4 mm and only a very limited white deposition was distributed and seen on the surface of the control mortar. These results were attributed to the chemical reaction between the $Ca(OH)_2$ leached from the concrete matrix to the surrounding carbon dioxide. In contrast, the artificial cracked bacterial mortar of 0.4 mm width was fully healed by microbial precipitation as shown in Fig. 8b. The microbial precipitation was later identified as vaterite and calcite ($CaCO_3$).

For the control mortar sample, the hydration product of the cement paste, calcium hydroxide is known as one of the main sources of calcium ions in concrete cracks. In addition, the carbondioxide in the air dissolved in water forming carbonate. Then, the carbonate formed diffused into the crack. As such, the carbonate would react with the free ions of calcium, forming calcium carbonate as shown in Eqs. (8) and (9). This result was in a good agreement with the present literature. For example [83], stated that only a crack width of 0.15 mm was fully healed by chemical calcium carbonate which was precipitated in the crack surface. In addition, [84] concluded that cement-based material has the ability to self-heal crack width ranging from 0.1 to 0.15 mm. According to them, this positive result was due to the continuous hydration of unhydrated cement particles and carbonation.

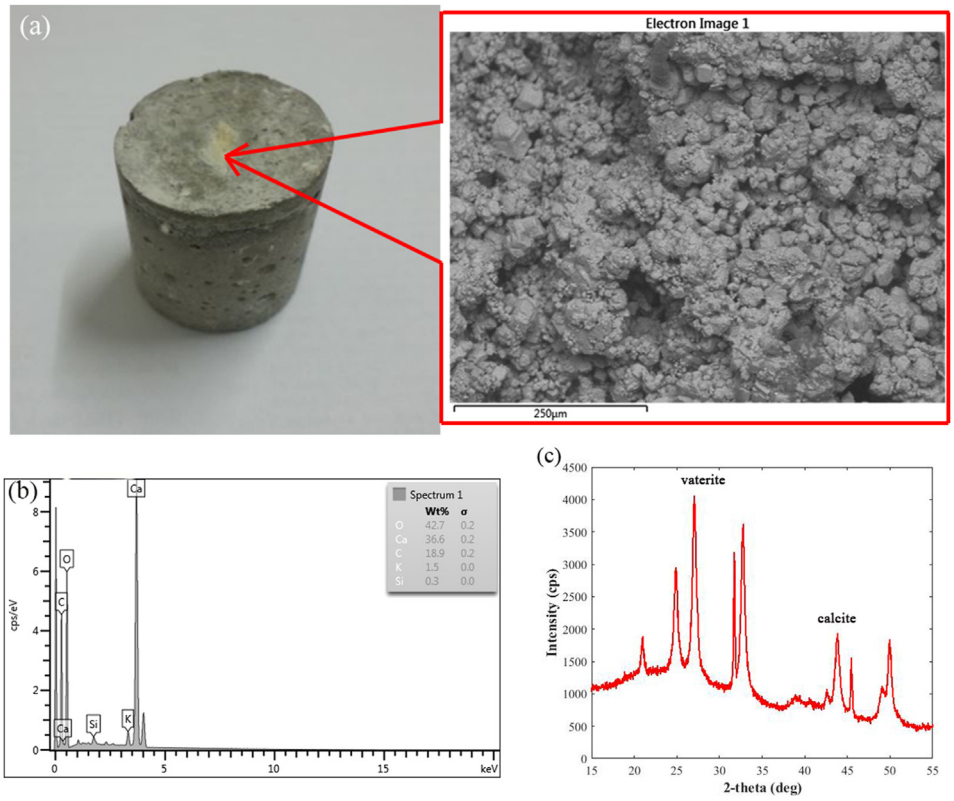

Fig. 10 – SEM-EDS and XRD analysis.

$$CaO + H_2O \rightarrow Ca(OH)_2 \quad (8)$$

$$Ca(OH)_2 + CO_2 \rightarrow CaCO_3 + H_2O \quad (9)$$

Back to the bacterial concrete, the crack-healing performance of the bacterial concrete samples was significantly enhanced in comparison to the control specimen owing to the formation of microbial calcium carbonate. Fig. 9 illustrates the precipitation of the microbial product in the crack surface of the bacterial concrete samples at different times using Variable Pressure Scanning Electron Microscopy (VP-SEM). It was observed that *pseudomycoides* strain HASS3 proved its ability to fully heal a crack width of 0.4 mm in just 68 days owing to their novel characteristic as discussed in section 3.1 and 3.2. This positive result enables *pseudomycoides* strain HASS3 to be one of the best bacterial species to heal concrete cracks compared to other bacterial species. For example, only a crack widths of 0.15–0.17 mm were completely healed using *B. sphaericus* species in a study reported by [85]. These results were almost in line with that of [53] who found that *Bacillus Subtilis* species has ability to only plug a 0.2 mm crack width. In addition, *B. megaterium* species showed its ability to plug a crack width of 0.3 mm at the age of 81 days in a study reported by [39]. In the same context, *Sporosarcina* pasteurii showed its capability to heal crack of up to 0.417 mm [86].

In the present study, it should be noted that the crack healing efficiency was evaluated by the decrease in the initial crack area h_i over time. Specifically, the initial crack area was subtracted from the crack area at interval time h_t divided by the initial area as expressed in Eq. (10).

$$h = \frac{h_i - h_t}{h_i} \times 100 \quad (10)$$

It was noticeable that the calcium carbonate precipitation started to appear along the edge of the crack surface as burrs. The microbial precipitation was clearly seen on the edge of both sides of the crack zone after 14 days as demonstrated in Fig. 9b. In addition, the healing ratio was just 6%. After that, the precipitation gradually increased over time. The improvement value depended on viability of urea and calcium which were necessary to establish the ureolytic activity. With more urea concentration, more calcium carbonate would be formed in the presence of the bacterial strain. Consequently, the microbial $CaCO_3$ precipitation continued until it bridged the full crack width. In particular, the cracked bio-mortar specimens were fully mended in 68 d, as illustrated in Fig. 9c. Such result proved that the crack surface could act as a suitable environment to promote the productivity of calcium carbonate as the pH value is low in the crack mouth. According to [64], the pH at the crack surface is between 9 and 11, whereas, the pH value may reach up to 13 inside the concrete matrix. In addition, the crack mouth is distinguished by the abundant oxygen from the surrounding. This oxygen is important for the growth of aerobic bacteria. With sufficient amount of oxygen and nutrient, the bacterial cell could multiply by binary fission and thus the number of cells would increase. In other words, the crack zone promotes the bacterial spore to transform into

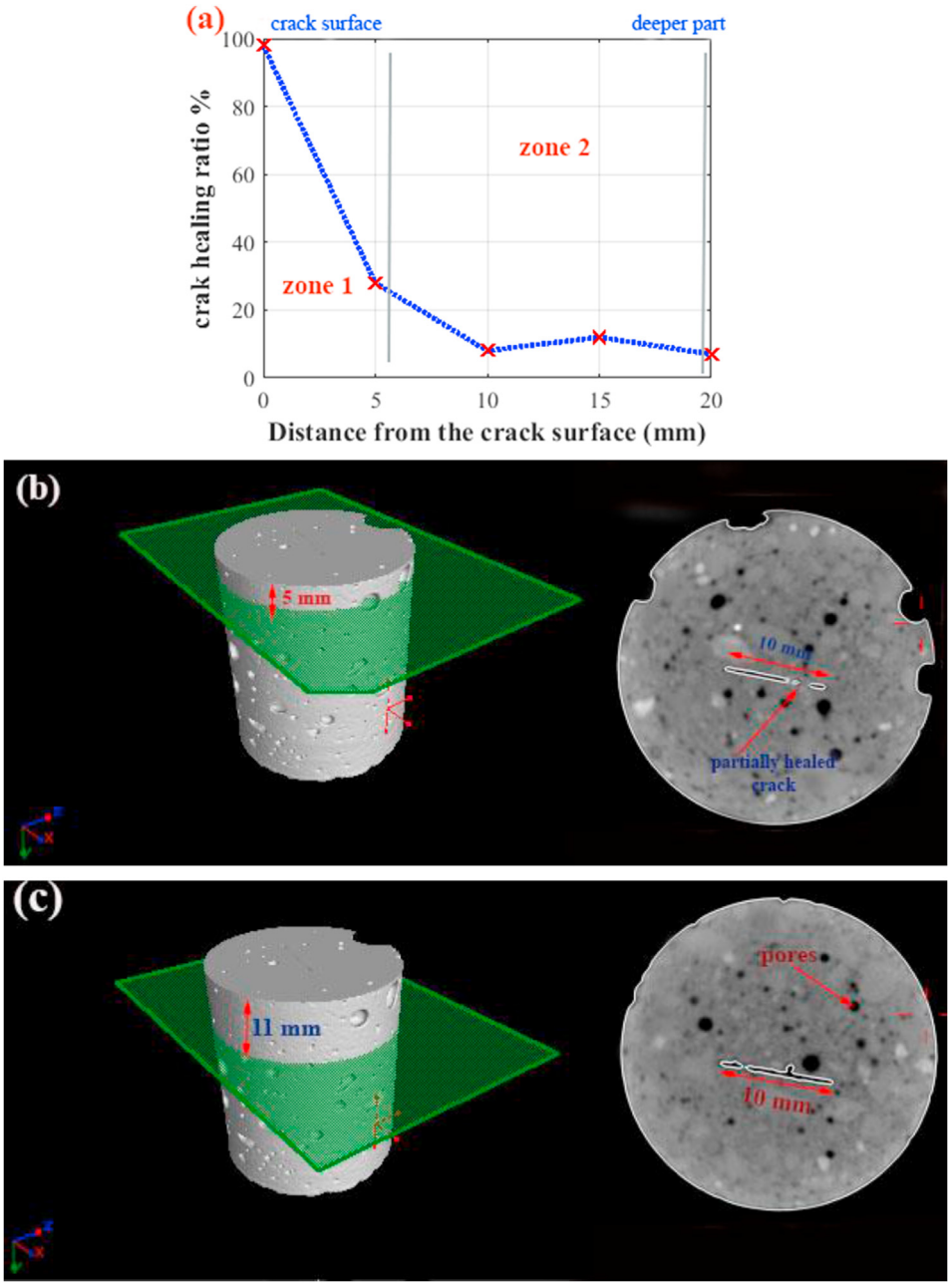

Fig. 11 – Horizontal cross sectional view from 3D x rays image of the artificial cracked bio-mortar specimen at different locations.

vegetative cell in just a few minutes due to favourable conditions, such as sufficient nutrient and pH of less than 12 [87]. This process is termed germination. During the germination process, the bacterial spore starts to elongate and then divide. Specifically, the bacteria cell grows again and subsequently, divides into two new vegetative daughter cells through binary fission. This process is very important to increase the number of bacterial cells. With more bacterial cells concentration, more carbonate ions could be produced, which is the main parameter to increase the precipitation of calcium carbonate.

From another point of view, it could be seen that the rate of crack healing was high during the early stage in comparison with the later stage as shown in Fig. 9d. Specifically, the slope of the healing ratio was higher during the first 28 days and it reduced slightly over time. This was because the enhancement of the healing ratio was dependent on the availability of the relevant materials such as urea and calcium. At a later age, the relevant chemical compounds were limited in the deeper part of crack mouth. These materials are necessary to complete the process of ureolytic activity as explained earlier. Another reason was that the viability of the bacteria was of great importance, in which it is faced with challenges that increases with time. In particular, the concrete pores acted as a space to host the bacterial cell. Over long period, the concrete matrix became denser, which might hit and crush the

bacterial cell. As a result, the bacteria could die, thus causing the number of bacteria to reduce over time. When the bacteria cells reduced, urea would become stable and would not convert into carbonate in the absence of the bacteria.

Moving on, the precipitated product on the crack surface was identified using XRD. Fig. 10c shows that the main product of the precipitation was vaterite, while the amount of calcite was limited in the present study. Vaterite was distinguished by its lower density in comparison to calcite in which it would occupy more space in the bacterial cementitious material [88]. As a result, the performance of the bacterial concrete was significantly enhanced. This result was consistent with many previous studies, which reported the different types of precipitation from different bacterial species. For example, [89] demonstrated that microbial calcium carbonate precipitation obtained from *B. amyloliquefaciens* were vaterite and calcite. According to them, the amount of vaterite was higher than calcite. In contrast, [82] concluded that the deposited crystal on the bacterial concrete crack corresponds to pure calcite according to the X-ray diffraction analysis. Such differences in the polymorphs of calcium carbonate might be attributed to factors such as temperature, pH, oversaturation and the ratio of calcium to carbonite ions [90]. According to [91], polymorphs of calcium carbonate were also dependent on urea concentration. In general, both calcite and vaterite are the main forms of calcium carbonate. Relatedly, the polymorphs of calcium carbonate are classified into two groups namely anhydrous crystalline and hydrated crystalline polymorphs. Argonite, calcite and vaterite are considered as anhydrous crystalline polymorphs [92]. On the contrary, hydrated crystalline polymorphs are calcium carbonate monohydrate ($CaCO_3.H_2O$) and calcium carbonate hexahydrate ($CaCO_3.6H_2O$) [93]. In addition, it can be inferred that both calcite and vaterite are the main forms of calcium carbonate in the precipitation of bacterial concrete.

Moreover, the morphology of the calcium carbonate precipitate on the crack surface obtained was observed with SEM analysis as shown in Fig. 10a. It could be seen that a majority of the precipitated was spherical shaped which belonged to vaterite. This fact was consistent with [94]. Based on their finding, the spheres shape of the bio-mineralisation was related to vaterite. It was also noticeable that the small precipitated crystal bonded with each other to form a larger size which is also known as bacterial aggregate. In addition, SEM-EDS (Fig. 10a and b) confirmed that the main elements of the precipitated were calcium (Ca), oxygen (O) and carbon (C) which revealed it is calcium carbonte $CaCO_3$.

On the other hand, X rays CT images presented an important insight into the amount of microbial precipitation in the deeper part of the crack zone. It is noteworthy that the amount of calcium carbonate precipitation in the deeper part was smaller than that of the crack mouth. Fig. 11 shows the 3D model of the artificial cracked mortar which was constructed using the VGStudio Max program. According to both the cross section views and gray levels, the healing ratio was simply calculated using Eq. (10) in which the dark region represented low density material such as void. Meanwhile, the bright region was related to high density material such as aggregate and cement paste. As such, it was significant that the porosity of the bio-concrete was location-dependent, in which the porosity in the deeper part was higher than the parts nearer to the surface. In addition, it could be seen that the healing ratio along the crack profile decreased as the distance from the crack surface increased, as shown in Fig. 11a. For instance, the healing ratio was approximately 28% at 5 mm depth from the surface, compared to that of at the crack mouth, as shown in Fig. 11b. In addition, the healing ratio decreased by up to 8% at 11 mm depth from the concrete surface, as demonstrated in Fig. 11c. Based on the obtained results, it could be summarised that the crack zone could be divided into two zones, according to the amount of calcium carbonate precipitation. The crack mouth represented the first zone, which approximately satisfied the optimum condition of the bacterial activity. This was because the crack mouth was affected by the surrounding environment such as available oxygen and pH of less than 11, as discussed earlier. The availability of oxygen would prompt the bacteria to germinate and then multiply, whereas the pH value of between 9 and 11 eased the ability of the bacteria to induce urease enzyme. Next, the second zone was represented by the deeper part of the crack. Zone 2 was distinguished by its high pH value. This was due to the available amount of calcium hydroxide inside the concrete matrix, which was responsible to increase pH, and thus, hindered the bacterial activity inside the concrete matrix. Indeed, [95] stated that ureolytic activity reduced by 80% in the pH of 12–13, as compared to a pH value of 9.

4. Conclusion

The high cost of rehabilitating deteriorated cementitious based structures has prompted the need to find and develop new techniques to overcome the said issues. Therefore, bacteria-based self-healing concrete has been extensively researched and utilised to overcome the propagation of microcracks through the precipitation of microbial calcium carbonate. In the present study, a new bacterial species, namely *B. pseudomycoides* species, was introduced and utilised to heal concrete crack width of 0.4 mm. X-ray μCT scan was taken into account to accurately monitor the healing ratio in the deeper part of the crack. Meanwhile, variable-pressure scanning electron microscope (VP-SEM) was used to measure the microbial precipitation in the crack surface. The result revealed that *pseudomycoides* strain HASS3 proved its ability to fully heal a crack width of 0.4 mm after 68 days, whereas, the healing ratio was limited in the deeper part. Therefore, it could be concluded that the effectiveness of the bacterial activity in the deeper parts of concrete still requires additional research prior to its real application. In other words, further studies are still needed to facilitate and enhance the efficiency of the bacteria activity inside the concrete matrix. Moreover, the interfacial transient zone (ITZ) of the bacterial concrete is also an interesting topic to be explored. In the same context, a predicative mathematical model is in demand in order to reduce both cost and time.

Declaration of Competing Interest

Authors declare no conflicts of interest.

Acknowledgment

The authors acknowledge full gratitude to Universiti Tun Hussein Onn Malaysia (UTHM) and Ministry of Higher Education through fundamental research grant scheme VOT. NO. FRGS/1/2018/TK01/UTHM/02/3. In addition, this research activity was also supported and funded by K122- Malaysian Technical University Grant(MTUN), Ministry Higher Education and M007- Industry Grant, PLUS BERHAD. Indeed, the authors would like to thank their support and cooperation in this research. Moreover, the authors extend their thanks to Shimadzu Corporation, Alex Corporation (M) Sdn Bhd (KS Wong) and Volume Graphic Software for their assistance and collaboration during the analysis of the X-Ray CT imaging using Shimadzu Inspexio SMX-225 CT Inspection System.

REFERENCES

[1] Jiang Z, Li J, Li W. Preparation and characterization of autolytic mineral microsphere for self-healing cementitious materials. Cement Concr Compos 2019;103:112–20. https://doi.org/10.1016/j.cemconcomp.2019.04.004.

[2] Xu J, Tang Y, Wang X, Wang Z, Yao W. Application of ureolysis-based microbial CaCO3 precipitation in self-healing of concrete and inhibition of reinforcement corrosion. Construct Build Mater 2020;265:120364. https://doi.org/10.1016/j.conbuildmat.2020.120364.

[3] Feng J, Dong H, Wang R, Su Y. A novel capsule by poly (ethylene glycol) granulation for self-healing concrete. Cement Concr Res 2020;133:106053. https://doi.org/10.1016/j.cemconres.2020.1060.

[4] Gökçe HS, Andiç-Çakır Ö. Bleeding characteristics of high consistency heavyweight concrete mixtures. Construct Build Mater 2019;194:153–60. https://doi.org/10.1016/j.conbuildmat.2018.11.029.

[5] Kayondo M, Combrinck R, Boshoff W. State-of-the-art review on plastic cracking of concrete. Construct Build Mater 2019;225:886–99. https://doi.org/10.1016/j.conbuildmat.2019.07.197.

[6] Algaifi HA, Bakar SA, Sam ARM, Abidin ARZ, Shahir S, AL-Towayti WAH. Numerical modeling for crack self-healing concrete by microbial calcium carbonate. Construct Build Mater 2018;189:816–24. https://doi.org/10.1016/j.conbuildmat.2018.08.218.

[7] Li K, Li L. Crack-altered durability properties and performance of structural concretes. Cement Concr Res 2019;124:105811. https://doi.org/10.1016/j.cemconres.2019.105811.

[8] Shah KW, Huseien GF. Biomimetic self-healing cementitious construction materials for smart buildings. Biomimetics 2020;5(4):47. https://doi.org/10.3390/biomimetics5040047.

[9] Kaur NP, Shah JK, Majhi S, Mukherjee A. Healing and simultaneous ultrasonic monitoring of cracks in concrete. Materials Today Communications 2019;18:87–99. https://doi.org/10.1016/j.mtcomm.2018.10.022.

[10] de Brito J, Kurda R. The past and future of sustainable concrete: a critical review and new strategies on cement-based materials. J Clean Prod 2020:123558. https://doi.org/10.1016/j.jclepro.2020.123558.

[11] El-Newihy A, Azarsa P, Gupta R, Biparva A. Effect of polypropylene fibers on self-healing and dynamic modulus of elasticity recovery of fiber reinforced concrete. Fibers 2018;6(1):9.

[12] Azarsa P, Gupta R, Biparva A. Assessment of self-healing and durability parameters of concretes incorporating crystalline admixtures and Portland Limestone Cement. Cement Concr Compos 2019;99:17–31.

[13] Byoungsun P, Young CC. Investigating a new method to assess the self-healing performance of hardened cement pastes containing supplementary cementitious materials and crystalline admixtures. J Mater Res Technol 2019;8(6):6058–73.

[14] Escoffres P, Desmettre C, Charron J-P. Effect of a crystalline admixture on the self-healing capability of high-performance fiber reinforced concretes in service conditions. Construct Build Mater 2018;173:763–74.

[15] Du W, Yu J, Gu Y, Li Y, Han X, Liu Q. Preparation and application of microcapsules containing toluene-di-isocyanate for self-healing of concrete. Construct Build Mater 2019;202:762–9.

[16] Van Belleghem B, Kessler S, Van den Heede P, Van Tittelboom K, De Belie N. Chloride induced reinforcement corrosion behavior in self-healing concrete with encapsulated polyurethane. Cement Concr Res 2018;113:130–9.

[17] Alshalif AF, Irwan J, Othman N, Al-Gheethi A, Shamsudin S, Nasser IM. Optimisation of carbon dioxide sequestration into bio-foamed concrete bricks pores using Bacillus tequilensis. J CO2 Utilization 2021;44:101412.

[18] Danish A, Mosaberpanah MA, Salim MU. Past and present techniques of self-healing in cementitious materials: a critical review on efficiency of implemented treatments. J Mater Res Technol 2020;9(3):6883–99.

[19] Balzano B, Sweeney J, Thompson G, Tuinea-Bobe C-L, Jefferson A. Enhanced concrete crack closure with hybrid shape memory polymer tendons. Eng Struct 2019;226:111330. https://doi.org/10.1016/j.engstruct.2020.111330.

[20] Qureshi T, Kanellopoulos A, Al-Tabbaa A. Autogenous self-healing of cement with expansive minerals-II: impact of age and the role of optimised expansive minerals in healing performance. Construct Build Mater 2019;194:266–75. https://doi.org/10.1016/j.conbuildmat.2018.11.027.

[21] Suleiman AR, Nelson AJ, Nehdi ML. Visualization and quantification of crack self-healing in cement-based materials incorporating different minerals. Cement Concr Compos 2019;103:49–58. https://doi.org/10.1016/j.cemconcomp.2019.04.026.

[22] He Z, Shen A, Guo Y, Lyu Z, Li D, Qin X, et al. Cement-based materials modified with superabsorbent polymers: a review. Construct Build Mater 2019;225:569–90. https://doi.org/10.1016/j.conbuildmat.2019.07.139.

[23] Lefever G, Snoeck D, Aggelis DG, De Belie N, Van Vlierberghe S, Van Hemelrijck D. Evaluation of the self-healing ability of mortar mixtures containing superabsorbent polymers and nanosilica. Materials 2020;13(2):380. https://doi.org/10.3390/ma13020380.

[24] Sidiq A, Gravina R, Setunge S, Giustozzi F. The effectiveness of Super Absorbent polymers and superplasticizer in self-healing of cementitious materials. Construct Build Mater 2020;253:119175. https://doi.org/10.1016/j.conbuildmat.2020.119175.

[25] Huseien GF, Shah KW, Sam ARM. Sustainability of nanomaterials based self-healing concrete: an all-inclusive insight. J. Build. Eng. 2019;23:155–71. https://doi.org/10.1016/j.jobe.2019.01.032.

[26] Olivier G, Combrinck R, Kayondo M, Boshoff WP. Combined effect of nano-silica, super absorbent polymers, and synthetic fibres on plastic shrinkage cracking in concrete. Construct Build Mater 2018;192:85–98. https://doi.org/10.1016/j.conbuildmat.2018.10.102.

[27] Teddy T, Irwan J, Othman N. The influence of sulphate reduction bacteria on the durability of concrete in seawater condition. Pertanika J Sci Technol 2017;25:117–22.
[28] Erşan YÇ, Hernandez-Sanabria E, Boon N, De Belie N. Enhanced crack closure performance of microbial mortar through nitrate reduction. Cement Concr Compos 2016;70:159–70. https://doi.org/10.1016/j.cemconcomp.2016.04.001.
[29] Erşan YÇ, Verbruggen H, De Graeve I, Verstraete W, De Belie N, Boon N. Nitrate reducing CaCO3 precipitating bacteria survive in mortar and inhibit steel corrosion. Cement Concr Res 2016;83:19–30. https://doi.org/10.1016/j.cemconres.2016.01.009.
[30] Jonkers HM, Thijssen A, Muyzer G, Copuroglu O, Schlangen E. Application of bacteria as self-healing agent for the development of sustainable concrete. Ecol Eng 2010;36(2):230–5. https://doi.org/10.1016/j.ecoleng.2008.12.036.
[31] Kaur NP, Majhi S, Dhami NK, Mukherjee A. Healing fine cracks in concrete with bacterial cement for an advanced non-destructive monitoring. Construct Build Mater 2020;242:118151. https://doi.org/10.1016/j.conbuildmat.2020.118151.
[32] Rauf M, Khaliq W, Khushnood RA, Ahmed I. Comparative performance of different bacteria immobilized in natural fibers for self-healing in concrete. Construct Build Mater 2020;258:119578. https://doi.org/10.1016/j.conbuildmat.2020.119578.
[33] Chaerun SK, Syarif R, Wattimena RK. Bacteria incorporated with calcium lactate pentahydrate to improve the mortar properties and self-healing occurrence. Sci Rep 2020;10(1):1–9. https://doi.org/10.1038/s41598-020-74127-4.
[34] Jongvivatsakul P, Janprasit K, Nuaklong P, Pungrasmi W, Likitlersuang S. Investigation of the crack healing performance in mortar using microbially induced calcium carbonate precipitation (MICP) method. Construct Build Mater 2019;212:737–44. https://doi.org/10.1016/j.conbuildmat.2019.04.035.
[35] Reddy BMS, Revathi D. An experimental study on effect of Bacillus sphaericus bacteria in crack filling and strength enhancement of concrete. Mater Today Proc 2019;19:803–9. https://doi.org/10.1016/j.matpr.2019.08.135.
[36] Khushnood RA, Qureshi ZA, Shaheen N, Ali S. Bio-mineralized self-healing recycled aggregate concrete for sustainable infrastructure. Sci Total Environ 2020;703:135007. https://doi.org/10.1016/j.scitotenv.2019.135007.
[37] Shahid S, Aslam MA, Ali S, Zameer M, Faisal M. "Self-Healing of cracks in concrete using Bacillus strains encapsulated in sodium alginate beads". Chemistry 2020;5(1):312–23. https://doi.org/10.1002/slct.201902206.
[38] Jafarnia MS, Saryazdi MK, Moshtaghioun SM. Use of bacteria for repairing cracks and improving properties of concrete containing limestone powder and natural zeolite. Construct Build Mater 2020;242:118059. https://doi.org/10.1016/j.conbuildmat.2020.118059.
[39] Krishnapriya S, Babu DV. Isolation and identification of bacteria to improve the strength of concrete. Microbiol Res 2015;174:48–55. https://doi.org/10.1016/j.micres.2015.03.009.
[40] González Á, Parraguez A, Corvalán L, Correa N, Castro J, Stuckrath C, et al. Evaluation of Portland and Pozzolanic cement on the self-healing of mortars with calcium lactate and bacteria. Construct Build Mater 2020;257:119558. https://doi.org/10.1016/j.conbuildmat.2020.119558.
[41] Jadhav UU, Lahoti M, Chen Z, Qiu J, Cao B, Yang E-H. Viability of bacterial spores and crack healing in bacteria-containing geopolymer. Construct Build Mater 2018;169:716–23. https://doi.org/10.1016/j.conbuildmat.2018.03.039.
[42] Singh H, Gupta R. Cellulose fiber as bacteria-carrier in mortar: self-healing quantification using UPV. J. Build. Eng. 2020;28:101090.
[43] Singh H, Gupta R. Influence of cellulose fiber addition on self-healing and water permeability of concrete. Case Studies in Construction Materials 2020;12:e00324.
[44] Son HM, Kim HY, Park SM, Lee HK. Ureolytic/non-ureolytic bacteria co-cultured self-healing agent for cementitious materials crack repair. Materials 2018;11(5):782. https://doi.org/10.3390/ma11050782.
[45] Wiktor V, Jonkers HM. Quantification of crack-healing in novel bacteria-based self-healing concrete. Cement Concr Compos 2011;33(7):763–70. https://doi.org/10.1016/j.cemconcomp.2011.03.012.
[46] Priya TS, Ramesh N, Agarwal A, Bhusnur S, Chaudhary K. Strength and durability characteristics of concrete made by micronized biomass silica and Bacteria-Bacillus sphaericus. Construct Build Mater 2019;226:827–38. https://doi.org/10.1016/j.conbuildmat.2019.07.172.
[47] Tayebani B, Mostofinejad D. Self-healing bacterial mortar with improved chloride permeability and electrical resistance. Construct Build Mater 2019;208:75–86. https://doi.org/10.1016/j.conbuildmat.2019.02.172.
[48] Wang J, Dewanckele J, Cnudde V, Van Vlierberghe S, Verstraete W, De Belie N. X-ray computed tomography proof of bacterial-based self-healing in concrete. Cement Concr Compos 2014;53:289–304. https://doi.org/10.1016/j.cemconcomp.2014.07.014.
[49] Zhang J, Liu Y, Feng T, Zhou M, Zhao L, Zhou A, et al. Immobilizing bacteria in expanded perlite for the crack self-healing in concrete. Construct Build Mater 2017;148:610–7. https://doi.org/10.1016/j.conbuildmat.2017.05.021.
[50] Bhaskar S, Hossain KMA, Lachemi M, Wolfaardt G, Kroukamp MO. Effect of self-healing on strength and durability of zeolite-immobilized bacterial cementitious mortar composites. Cement Concr Compos 2017;82:23–33. https://doi.org/10.1016/j.cemconcomp.2017.05.013.
[51] Jogi PK, Lakshmi TV. Self healing concrete based on different bacteria: a review. Mater Today Proc 2020. https://doi.org/10.1016/j.matpr.2020.08.765.
[52] Joshi S, Goyal S, Mukherjee A, Reddy MS. Microbial healing of cracks in concrete: a review. J Ind Microbiol Biotechnol 2017;44(11):1511–25. https://doi.org/10.1007/s10295-017-1978-0.
[53] Kalhori H, Bagherpour R. Application of carbonate precipitating bacteria for improving properties and repairing cracks of shotcrete. Construct Build Mater 2017;148:249–60. https://doi.org/10.1016/j.conbuildmat.2017.05.074.
[54] Khaliq W, Ehsan MB. Crack healing in concrete using various bio influenced self-healing techniques. Construct Build Mater 2016;102:349–57. https://doi.org/10.1016/j.conbuildmat.2015.11.006.
[55] Li L, Zheng Q, Li Z, Ashour A, Han B. Bacterial technology-enabled cementitious composites: a review. Compos Struct 2019;225:111170. https://doi.org/10.1016/j.compstruct.2019.111170.
[56] Mondal S, Ghosh AD. Review on microbial induced calcite precipitation mechanisms leading to bacterial selection for microbial concrete. Construct Build Mater 2019;225:67–75. https://doi.org/10.1016/j.conbuildmat.2019.07.122.
[57] Qian C, Chen H, Ren L, Luo M. Self-healing of early age cracks in cement-based materials by mineralization of carbonic anhydrase microorganism. Front Microbiol 2015;6:1225. https://doi.org/10.3389/fmicb.2015.01225.

[58] Reddy PY, Ramesh B, Kumar LP. Influence of bacteria in self healing of concrete-a review. Mater Today Proc 2020. https://doi.org/10.1016/j.matpr.2020.07.233.
[59] Sidiq A, Gravina R, Giustozzi F. Is concrete healing really efficient? A review. Construct Build Mater 2019;205:257–73. https://doi.org/10.1016/j.conbuildmat.2019.02.002.
[60] Welton R, Silva MR, Gaylarde C, Herrera L, Anleo X, De Belie N, et al. Techniques applied to the study of microbial impact on building materials. Mater Struct 2005;38(10):883–93.
[61] Balam NH, Mostofinejad D, Eftekhar M. Effects of bacterial remediation on compressive strength, water absorption, and chloride permeability of lightweight aggregate concrete. Construct Build Mater 2017;145:107–16. https://doi.org/10.1016/j.conbuildmat.2017.04.003.
[62] Hamid MAA, Aziz HA, Yusoff MS, Rezan SA. Optimization and analysis of zeolite augmented electrocoagulation process in the reduction of high-strength ammonia in saline landfill leachate. Water 2020;12(1):247.
[63] Zhao X, Yin F, Liu N, Li G, Fan T, Chen B. "Highly efficient metal–organic-framework catalysts for electrochemical synthesis of ammonia from N 2 (air) and water at low temperature and ambient pressure". J Mater Sci 2017;52(17):10175–85.
[64] Wang J, Jonkers HM, Boon N, De Belie N. Bacillus sphaericus LMG 22257 is physiologically suitable for self-healing concrete. Appl Microbiol Biotechnol 2017;101(12):5101–14. https://doi.org/10.1007/s00253-017-8260-2.
[65] Derakshani M, Lukow T, Liesack W. Novel bacterial lineages at the (sub) division level as detected by signature nucleotide-targeted recovery of 16S rRNA genes from bulk soil and rice roots of flooded rice microcosms. Appl Environ Microbiol 2001;67(2):623–31. https://doi.org/10.1128/AEM.67.2.623-631.2001.
[66] Ramachandran SK, Ramakrishnan V, Bang SS. Remediation of concrete using micro-organisms. ACI Mater J Am Concrete Institute 2001;98(1):3–9.
[67] Andalib R, Majid MZA, Hussin MW, Ponraj M, Keyvanfar A, Mirza J, et al. Optimum concentration of Bacillus megaterium for strengthening structural concrete. Construct Build Mater 2016;118:180–93. https://doi.org/10.1016/j.conbuildmat.2016.04.142.
[68] Veys-Behbahani R, Sharififard M, Dinparast-Djadid N, Shamsi J, Fakoorziba MR. Laboratory evolution of the entomopathogenic fungus Beauveria bassiana against Anopheles stephensi larvae (Diptera: Culicidae). Asian Pacific Journal of Tropical Disease 2014;4:S799–802. https://doi.org/10.1016/S2222-1808(14)60730-1.
[69] Stratford JP, Woodley MA, Park S. Variation in the morphology of Bacillus mycoides due to applied force and substrate structure. PloS One 2013;8(12):e81549. https://doi.org/10.1371/journal.pone.0081549.
[70] Beveridge TJ. Use of the Gram stain in microbiology. Biotech Histochem 2001;76(3):111–8. https://doi.org/10.1080/bih.76.3.111.118.
[71] Xu H, Lian J, Gao M, Fu D, Yan Y. Self-healing concrete using rubber particles to immobilize bacterial spores. Materials 2019;12(14):2313. https://doi.org/10.3390/ma12142313.
[72] Luo M, Qian C-x, Li R-y. Factors affecting crack repairing capacity of bacteria-based self-healing concrete. Construct Build Mater 2015;87:1–7. https://doi.org/10.1016/j.conbuildmat.2015.03.117.
[73] Okwadha GD, Li J. Optimum conditions for microbial carbonate precipitation. Chemosphere 2010;81(9):1143–8. https://doi.org/10.1016/j.chemosphere.2010.09.066.
[74] Krajewska B, Ciurli S. "Jack bean (Canavalia ensiformis) urease. Probing acid–base groups of the active site by pH variation". Plant Physiol Biochem 2005;43(7):651–8. https://doi.org/10.1016/j.plaphy.2005.05.009.
[75] Bundur ZB, Amiri A, Ersan YC, Boon N, De Belie N. Impact of air entraining admixtures on biogenic calcium carbonate precipitation and bacterial viability. Cement Concr Res 2017;98:44–9. https://doi.org/10.1016/j.cemconres.2017.04.005.
[76] Rahimpour M. A non-ideal rate-based model for industrial urea thermal hydrolyser. Chem Eng Process: Process Intensification 2004;43(10):1299–307. https://doi.org/10.1016/j.cep.2003.12.005.
[77] Erşan YÇ, De Belie N, Boon N. Microbially induced CaCO3 precipitation through denitrification: an optimization study in minimal nutrient environment. Biochem Eng J 2015;101:108–18.
[78] Tydlitát V, Matas T, Černý R. Effect of w/c and temperature on the early-stage hydration heat development in Portland-limestone cement. Construct Build Mater 2014;50:140–7.
[79] Vashisht R, Attri S, Sharma D, Shukla A, Goel G. Monitoring biocalcification potential of Lysinibacillus sp. isolated from alluvial soils for improved compressive strength of concrete. Microbiol Res 2018;207:226–31. https://doi.org/10.1016/j.micres.2017.12.010.
[80] Nain N, Surabhi R, Yathish N, Krishnamurthy V, Deepa T, Tharannum S. Enhancement in strength parameters of concrete by application of Bacillus bacteria. Construct Build Mater 2019;202:904–8. https://doi.org/10.1016/j.conbuildmat.2019.01.059.
[81] Lee YS, Park W. Current challenges and future directions for bacterial self-healing concrete. Appl Microbiol Biotechnol 2018;102(7):3059–70. https://doi.org/10.1007/s00253-018-8830-y.
[82] Jiang L, Jia G, Jiang C, Li Z. Sugar-coated expanded perlite as a bacterial carrier for crack-healing concrete applications. Construct Build Mater 2020;232:117222. https://doi.org/10.1016/j.conbuildmat.2019.117222.
[83] Sisomphon K, Copuroglu O, Koenders E. Self-healing of surface cracks in mortars with expansive additive and crystalline additive. Cement Concr Compos 2012;34(4):566–74. https://doi.org/10.1016/j.cemconcomp.2012.01.005.
[84] De Belie N, Gruyaert E, Al-Tabbaa A, Antonaci P, Baera C, Bajare D, et al. "A review of self-healing concrete for damage management of structures". Advanced materials interfaces 2018;5(17):1800074. https://doi.org/10.1002/admi.201800074.
[85] Wang J, Van Tittelboom K, De Belie N, Verstraete W. Use of silica gel or polyurethane immobilized bacteria for self-healing concrete. Construct Build Mater 2012;26(1):532–40.
[86] Xu J, Wang X. Self-healing of concrete cracks by use of bacteria-containing low alkali cementitious material. Construct Build Mater 2018;167:1–14.
[87] Foster S. "The role and regulation of cell wall structural dynamics during differentiation of endospore-forming bacteria". J Appl Bacteriol 1994;76:25S–39S. https://doi.org/10.1111/j.1365-2672.1994.tb04355.x.
[88] Seifan M, Samani AK, Berenjian A. Induced calcium carbonate precipitation using Bacillus species. Appl Microbiol Biotechnol 2016;100(23):9895–906. https://doi.org/10.1007/s00253-016-7701-7.
[89] Merve T, Arslan Ş, Koralay T, Doğan NM. Precipitation and characterization of CaCO3 of Bacillus amyloliquefaciens U17 strain producing urease and carbonic anhydrase. Turk J Biol 2019;43(3):198.
[90] Mitchell AC, Ferris FG. The influence of Bacillus pasteurii on the nucleation and growth of calcium carbonate. Geomicrobiol J 2006;23(3–4):213–26. https://doi.org/10.1080/01490450600724233.

[91] Işık M, Altaş L, Özcan S, Şimşek İ, Ağdağ ON, Alaş A. Effect of urea concentration on microbial Ca precipitation. J Ind Eng Chem 2012;18(6):1908–11. https://doi.org/10.1016/j.jiec.2012.05.002.
[92] Arias D, Cisternas LA, Rivas M. Biomineralization mediated by ureolytic bacteria applied to water treatment: a review. Crystals 2017;7(11):345. https://doi.org/10.3390/cryst7110345.
[93] Meldrum F. Calcium carbonate in biomineralisation and biomimetic chemistry. Int Mater Rev 2003;48(3):187–224. https://doi.org/10.1179/095066003225005836.
[94] Al-Thawadi S, Cord-Ruwisch R. Calcium carbonate crystals formation by ureolytic bacteria isolated from Australian soil and sludge. Adv Sci Eng Res 2012;2(1):12–26.
[95] Algaifi HA, Bakar SA, Sam ARM, Ismail M, Abidin ARZ, Shahir S, et al. Insight into the role of microbial calcium carbonate and the factors involved in self-healing concrete. Construct Build Mater 2020;254:119258. https://doi.org/10.1016/j.conbuildmat.2020.119258.